JOURNAL OF APPLIED ELECTROCHEMISTRY 26 (1996) 1259–1265

A synergistic effect between zinc salt and phosphonic acid for corrosion inhibition of a carbon steel

Y. GONZALEZ, M. C. LAFONT, N. PEBERE

U.R.A. CNRS 445, Laboratoire des Matériaux, Equipe de Métallurgie Physique, ENSCT, 118 Route de Narbonne, 31077 Toulouse Cedex, France

F. MORAN

Concorde Chimie France, 118, Avenue du Docteur Rosenfeld, 93230 Romainville, France

Received 14 September 1995; revised 22 February 1996

This work is devoted to the corrosion inhibition of a carbon steel by a zinc salt/phosphonic acid association. Steady-state current–voltage curves and electrochemical impedance measurements carried out in the presence of each compound and for the mixture show a synergistic effect between the two molecules. The concentrations of the compounds in the mixture were lower than the concentrations used for each compound separately. Phosphonic acid was observed to act as an anodic inhibitor whereas cathodic action was shown for the zinc chloride. Electrochemical measurements and surface analysis (XPS and reflection–adsorption spectroscopy at grazing incidence) showed that the synergistic effect afforded by the mixture was attributable to the reaction of the phosphonic acid with the zinc salt. The inhibitor film acts as a protective layer impermeable to ionic or molecular diffusion. The film is very thin and homogeneous in composition. A chemical structure of the film is proposed.

1. Introduction

The prevention of corrosion and scaling in cooling water systems is often achieved by the addition of inorganic or organic phosphorus compounds in association with zinc salts and low molecular weight polymers.

In a previous work [1], we demonstrated that a multicomponent inhibitor (a mixture of a phosphonic acid with a zinc salt) is very efficient as an inhibitor for the corrosion of a carbon steel, even at low concentrations (50 mg dm^{-3}). Between 50 and 200 mg dm^{-3}, the inhibitive efficiency increases from 95 to 98%. For 100 mg dm^{-3} it is effective over a wide pH range (5.5 to 9) with a better protection for pH 7 and pH 8. This first study was carried out in a 0.0034 M NaCl solution (the low electrical conductivity of this medium is close to that encountered in natural saline waters).

Recently, a study was carried out with the same inhibitive mixture in a 0.5 M NaCl solution [2] (in order to avoid the problems linked to the ohmic drop [3]). By combining the polarization curves and electrochemical impedance measurements, it was shown that the inhibitor forms a compact layer, impermeable to ionic and molecular diffusion. Corrosion proceeds only through small defects of the inhibitor film. In the medium studied, the inhibitive efficiency was estimated at around 98%. XPS analysis revealed the thinness of the film which is composed essentially of Zn, P and O. Formation of an iron oxide under the inhibitor layer was observed. In addition, infrared spectra of the film at grazing incidence were consistent with the reaction of the phosphonic acid with the zinc salt and the iron oxide to produce metal salts.

The aim of the present study was to obtain a better understanding of the mode of action of this inhibitive mixture through the knowledge of the structure of the surface film and through the study of the action of each of the constituents. As a matter of fact, studies have been reported in the literature on the synergistic effect of phosphonic acids and zinc salts in corrosion inhibition of mild steel in neutral medium [4, 5]. Nevertheless, this effect is not well understood. In the present study, steady-state current–voltage curves were combined with electrochemical impedance measurements in the presence of amino-trimethyl phosphonic acid (ATMP) or zinc chloride (majority constituents of the mixture) for various pH values of the 0.5 M sodium chloride solution (7, 8, 9 and 10). To our knowledge, the influence of the pH of the solutions on the inhibitive action of ATMP and zinc chloride has not been described in the literature.

2. Experimental details

2.1. *Material*

The sample selected for the study was an XC35 carbon steel and had the following composition in percent weight: C = 0.35, Mn = 0.65, Si = 0.25, P = 0.035,

0021-891X © 1996 Chapman & Hall

S = 0.035 and Fe to 100. For all the experiments, the carbon steel samples were polished with diamond paste (3 μm), cleaned in demineralized water in an ultrasonic bath for a few minutes to remove the polishing residues and then dried in warm air. The corrosion medium was a 0.5 M solution of NaCl (reagent grade) in contact with air maintained at 25 °C. The pH was adjusted by NaOH.

The inhibitor mixture tested was based on an amino-trimethyl phosphonic acid (ATMP) in combination with zinc chloride and small amounts of polyphosphates. All the measurements were carried out at a concentration of 500 mg dm^{-3} of the solution containing the compounds. For the compounds tested separately, it was necessary to increase the concentration to have sufficient protection. Thus, zinc chloride was tested at a concentration twice as high as in the mixture and for ATMP the concentration tested was ten times higher than in the mixture.

2.2. *Electrochemical measurements*

The working electrode was a rotating disk consisting of a carbon steel rod of 1 cm^2 cross-sectional area. A thermoretractable sheath preventing the cylindrical area from making contact with the solution, the electrode surface was only the cross section. All the experiments were carried out with a rotation rate of 1000 rpm. A saturated calomel electrode (SCE) was used as reference, it was placed far enough from the disc surface to avoid distortion in potential and velocity distributions; the auxiliary electrode was a platinum grid with a large surface area.

The ohmic drop in the electrolyte was small due to high conductivity of the sodium chloride solution; as a consequence, the polarization curves were obtained without ohmic drop compensation.

Electrochemical measurements were carried out using a Solartron Schlumberger 1250 frequency response analyser with a Solartron 1286 electrochemical interface. The data were processed by a Hewlett Packard 9000 computer.

2.3. *Infrared spectroscopy*

Over the range 4000–750 cm^{-1} Fourier transform infrared spectra were obtained at 2 cm^{-1} resolution on a Perkin Elmer 1760X spectrometer. The spectra of the compounds in solution were obtained by transmission. A model SPECAC grazing incidence spectrometer was used to study the metal surfaces. Measurements were made at an angle of 85°.

2.4. *XPS analysis*

The XPS measurements were performed with an electron spectrometer ESCALAB–MKII (VG scientific apparatus). The specimens were irradiated with the AlK_α ray source ($h\nu$ = 1486.6 eV). The X-ray power was 300 W. Angle-resolved measurements were made at a take-off angle $\theta = 90°$. Sputtering of the sample surface was performed with an argon ion gun under an accelerating voltage of 4 kV and a current density of approximately 75 μA cm^{-2}. All the samples were cleaned by ion sputtering for 2 min before the analysis.

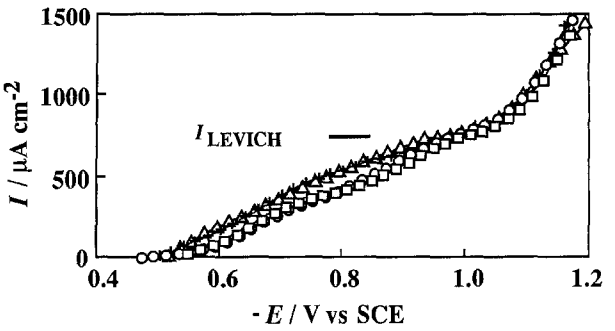

Fig. 1. Cathodic current–voltage curves obtained at different pH in the presence of ATMP after 2 h of immersion at E_{corr}. pH values: (△) 7; (+) 8; (□) 9; (○) 10.

3. Results and discussion

3.1. *Electrochemical results obtained in the presence of ATMP*

Figure 1 reports the steady-state cathodic polarization curves obtained for different solution pH in the presence of ATMP. The curves were weakly dependent on the solution pH over the whole potential range studied. Nevertheless, around the corrosion potential, the current densities were lower when the pH increased and a shift of E_{corr} occurred towards more anodic potentials (60 mV). Around −1 V a diffusion plateau was observed whatever the pH. Referring to analysis carried out previously [6, 7], we ascribe this plateau to the reduction of dissolved oxygen. The measured value of the limiting current density was not very different from that predicted by Levich [8] for a uniformly active surface (720 μA cm^{-2}). These observations suggest that ATMP acts only on the anodic sites.

Corrosion current densities can be determined from steady-state current–voltage curves. In the absence of inhibitor in solution, only diffusional control is observed [2], but with inhibitor a mixed activation and diffusion control occurs near the corrosion potential. These latter reaction kinetics are taken into account in the determination of the corrosion rates: corrosion current density (I_{corr}) was obtained by

Table 1. Parameters deduced from the cathodic current–voltage curves and electrochemical impedance diagrams at different pH values in the presence of ATMP

pH	E_{corr} /V vs SCE	I_{corr} /μA cm^{-2}	R_p /Ω cm^2	C /μF cm^{-2}
7	−0.496 ± 0.032	130 ± 50	410 ± 140	780 ± 580
8	−0.486 ± 0.016	74 ± 24	750 ± 85	430 ± 140
9	−0.504 ± 0.044	63 ± 67	1190 ± 270	240 ± 40
10	−0.496 ± 0.030	44 ± 26	3500 ± 1000	150 ± 60

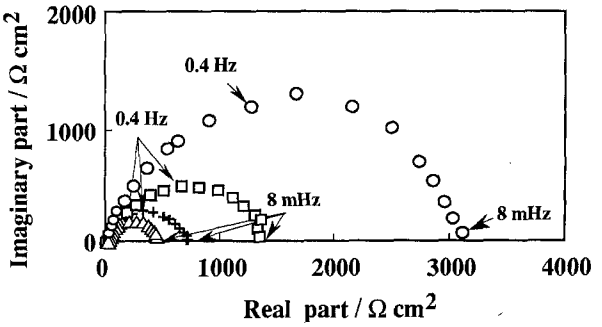

Fig. 2. Electrochemical impedance diagrams obtained at different pH in the presence of ATMP after 2 h of immersion at E_{corr}. pH values: (△) 7; (+) 8; (□) 9; (○) 10.

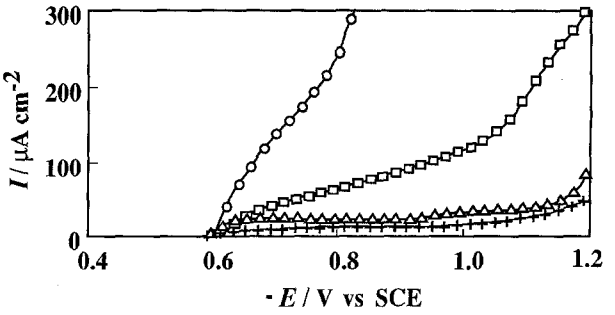

Fig. 3. Cathodic current–voltage curves obtained at different pH in the presence of zinc chloride after 2 h of immersion at E_{corr}. pH values: (△) 7; (+) 8; (□) 9; (○) 10.

back extrapolation to the corrosion potential of diffusion-corrected Tafel lines. The results obtained are reported in Table 1; their accuracy takes into account the dispersion over three trials. Examination of this table shows that I_{corr} significantly decreased when the pH rose from 7 to 10.

Figure 2 reports the impedance diagrams plotted at the corrosion potential for different solution pH in the presence of ATMP. The impedance diagrams are characterized by a single time constant. Comparison of the polarization resistance values determined from this loop (Table 1) corroborates the better protection of the material when the solution pH increases. In addition, the values of the resistance are significantly higher than those obtained for the blank solution.

The capacitance values associated with the capacitive loop are reported in Table 1. A decrease in the capacitance values is observed with increase in pH. For the solution without inhibitor, the capacitance was around 1 mF cm^{-2}. This is higher than the usual value of the double layer capacitance (50 μF cm^{-2}). Duprat *et al.* [9] have shown that the high value is due to a large increase in the specific area caused by the presence of the corrosion products on the metallic surface. Thus, for ATMP, the decrease in the capacitance can be explained by a decrease in the quantity of the corrosion product due to the increase in the inhibitive effect with pH.

From the electrochemical results obtained, and in agreement with data from the literature, a mechanism for the inhibitive action of ATMP can be proposed. This compound has the property to form insoluble chelates [10] with bivalent metal ions (Ca^{2+}, Fe^{2+}, Zn^{2+}, Mg^{2+}). Equation 1 shows that the presence of hydroxide ions shifts the neutral form of the molecule towards the ionic form. The ionic form combines with the Fe^{2+} ions to give the corresponding chelate (Equation 2):

$$(C_3H_6NP_3O_9)^{6-}H^{6+} + 6\,OH^- = (C_3H_6NP_3O_9)^{6-} + 6\,H_2O \quad (1)$$

$$(C_3H_6NP_3O_9)^{6-} + 3\,Fe^{2+} = (C_3H_6NP_3O_9)^{6-}(Fe^{2+})_3 \quad (2)$$

When the pH of the solution becomes more basic, the formation of the complex on the steel surface is favoured. This mechanism involves the metal ions released during the anodic reaction. This leads to a decrease in the area available for this reaction and, consequently, to a decrease in the corrosion rate. This mechanism explains the anodic action of the molecule. This result is in agreement with the work of Kalman *et al.* [11]. These authors have shown that 1-hydro-ethane-1,1-diphosphonic acid (HEDP) has no effect on the cathodic oxygen reduction reaction and inhibits carbon steel corrosion by a precipitation mechanism forming insoluble iron complexes. Nevertheless, they mentioned that increasing HEDP concentration decreases its inhibition efficiency due to the dissolution of the oxide layer.

3.2. *Electrochemical results obtained in the presence of $ZnCl_2$*

The steady-state cathodic polarization curves obtained for solutions of various pH in the presence of zinc chloride are presented in Fig. 3. The curves have a similar shape for pH 7 and 8. They are characterized by the appearance of a current plateau. The height of the plateau was low in comparison with that of the solution without inhibitor [2]. This decrease is accounted for by the well-known cathodic action of the zinc chloride. The inhibitive action of zinc salt is attributed to the precipitation of a zinc hydroxide complex on the cathodic zones caused by a local increase in pH due to oxygen reduction [12]. The reactions are:

$$O_2 + 2H_2O + 4e^- = 4\,OH^- \quad (3)$$

$$Zn^{2+} + 2\,OH^- = Zn(OH)_2 \quad (4)$$

For pH 9 and 10, the cathodic current densities increase significantly. In the high pH region, Hitchman *et al.* [12] mentioned the dissolution of $Zn(OH)_2$ by the formation of a soluble zincate: $Zn(OH)_4^{2-}$ following the reaction:

$$Zn(OH)_2 + 2\,OH^- = Zn(OH)_4^{2-} \quad (5)$$

This may give rise to a porous structure and can explain the significant increase in the current densities at pH 10. The increase in pH has an unfavourable effect on the corrosion protection of steel; a severe attack of the steel surface was observed for the highest

Table 2. Parameters deduced from the cathodic current–voltage curves and electrochemical impedance diagrams at different pH values in the presence of zinc chloride

pH	E_{corr}/ V vs SCE	I_{corr} /μA cm^{-2}	*Rp* /Ω cm^2
7	-0.597 ± 0.004	19 ± 3	920 ± 130
8	-0.583 ± 0.008	15 ± 3	1500 ± 500
9	-0.584 ± 0.084	35 ± 10	580 ± 270
10	-0.594 ± 0.017	350 ± 50	470 ± 390

pH value. In this case, corrosion products appear all over the surface whereas, for the other pH values, they were unevenly deposited over the steel surface. Whatever the pH, it is observed that corrosion was initiated by pitting and spread out in the form of corrosion products. A significant increase in the size and depth of the pits was observed for a pH of 10.

The measurement of the corrosion rate in the presence of zinc chloride is not as straightforward. For the solutions of pH of 7 and 8, the corrosion current densities can be considered as equal to the limiting current. For pH 9 and 10, I_{corr} is estimated to be approximately the same as the value of the current density for a potential of -0.9 V. The values are reported in Table 2. The I_{corr} value was high for a pH of 10. It decreased for pH 9 and became low (15–20 μA cm^{-2}) for pH of 7 and 8. These results are in agreement with the visual observations of the surface.

Figure 4 presents the impedance diagrams obtained at the corrosion potential for different solution pH values in the presence of zinc chloride. The diagrams present a single distorted loop. For a pH of 8, the value of the polarization resistance was the highest and, conversely, for a pH of 10 the value was the lowest. This result corroborates those obtained from steady-state measurements. The increase in pH favours the dissolution of zinc hydroxide formed on the cathodic zones which leads to an increase in the current on the polarization curves and to a decrease in the polarization resistance.

3.3. *Electrochemical results obtained in the presence of the mixture*

Figure 5 shows the effect of pH on the cathodic polarization curves in the presence of the inhibitive

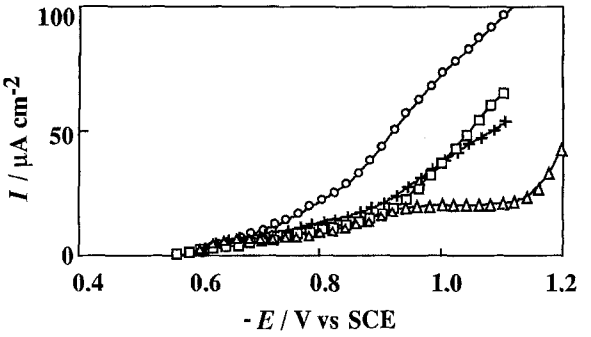

Fig. 5. Cathodic current–voltage curves obtained at different pH in the presence of the inhibitive mixture after 2 h of immersion at E_{corr}. pH values: (△) 7; (+) 8; (□) 9; (○) 10.

mixture. In the vicinity of the corrosion potential, the curves are independent of pH. The current densities were lower than when the compounds were tested alone. It must be emphasized that the concentrations of the compounds in the mixture were lower than the concentrations used for each compound. In addition, the corrosion potentials were slightly shifted anodically in comparison with the solution containing ATMP. For the curve obtained at pH 7, a very well-defined plateau is observed for potentials between -0.9 V and -1.1 V. For this potential region, the current densities increased with pH and there was a tendency for the plateau to disappear. This result seems to be linked to the presence of $ZnCl_2$ and to the dissolution of $Zn(OH)_2$. From these steady-state polarization curves, the synergic effect between ATMP and $ZnCl_2$ is clear and it is shown that the mixture is efficient over a wide pH range.

Whatever the pH, the electrode surface remained undamaged, bright and without corrosion products. Conversely, the surface observed after immersion in the solution in the presence of each compound separately, was attacked to varying extents according to the pH of the solution.

The impedance diagrams obtained at the corrosion potential in the presence of the mixture for different pH values present a single, rather flattened capacitive loop (Fig. 6). The value of the polarization resistance (Table 3) was high in comparison with those obtained with the separate compounds (Tables 1 and 2). The capacitance values calculated from the resistance and the characteristic frequencies varied from 100 to 300 μF cm^{-2}. They were weakly dependent on the pH.

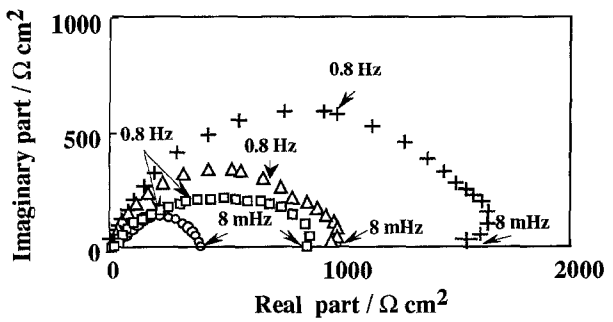

Fig. 4. Electrochemical impedance diagrams obtained at different pH in the presence of zinc chloride after 2 h of immersion at E_{corr}. pH values: (△) 7; (+) 8; (□) 9; (○) 10.

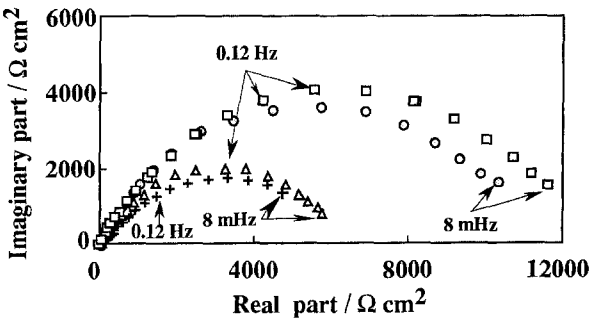

Fig. 6. Electrochemical impedance diagrams obtained at different pH in the presence of the inhibitive mixture after 2 h of immersion at E_{corr}. pH values: (△) 7; (+) 8; (□) 9; (○) 10.

Table 3. Parameters deduced from the electrochemical impedance diagrams at different pH values in the presence of the inhibitive mixture

pH	$Rp/\Omega\,cm^2$	$C/\mu F\,cm^2$
7	5100 ± 1600	220 ± 110
8	6500 ± 1500	240 ± 150
9	13100 ± 100	120 ± 30
10	11300 ± 5200	220 ± 100

The values of the polarization resistance are in agreement with the local slope of the current–voltage curve. The increase in the resistance for pH values of 9 and 10 is thought to be related to the action of ATMP according to the mechanism proposed previously. These results allow us to conclude that around the corrosion potential ATMP acts significantly in the corrosion inhibition of steel.

3.4. *Study of the synergistic effect*

Figure 7 reports, for comparison, the cathodic polarization curves obtained in the presence of ATMP, zinc chloride and the mixture for a pH of 7. These curves are a reminder that the very low current densities measured in the presence of the mixture are due to the action of zinc chloride. In the presence of ATMP, the shift of E_{corr} in the anodic direction as well as the high values of the current densities in comparison with the solution without inhibitor indicates the anodic action of the inhibitor.

Figure 8 presents the impedance diagrams plotted in Bode coordinates at the corrosion potential (pH 7), in the presence of ATMP, zinc chloride and the mixture. The diagram obtained without inhibitor is also presented.

The polarization resistance values obtained in the presence of each compound were higher than those obtained without inhibitor. For the mixture, the value was significantly increased. For ATMP, the shape of the diagram clearly reveals a single time constant. The results of Kalman [11] obtained by electrochemical impedance spectroscopy in the presence of HEDP have shown the presence of two time constants attributed to the presence of nonhomogeneous surface layer.

For zinc chloride, the phase angle is distorted, particularly in the high frequency domain. For the mixture, the occurrence of two time constants can be hypothesized owing to the large peak obtained for the phase angle (Fig. 8). This is corroborated by the fact that the impedance diagrams obtained for different immersion times reveal two time constants [2].

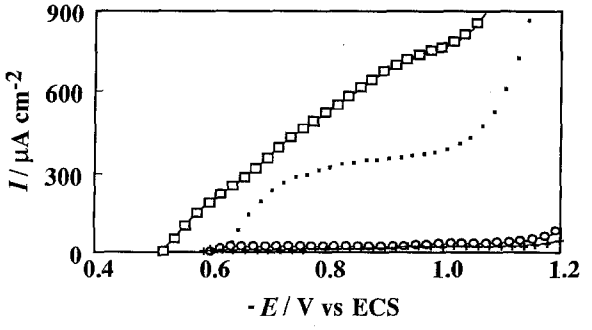

Fig. 7. Cathodic current–voltage curves obtained at pH 9 in the presence of: (□) ATMP; (○) $ZnCl_2$; (+) the inhibitive mixture; (■■■■) without inhibitor.

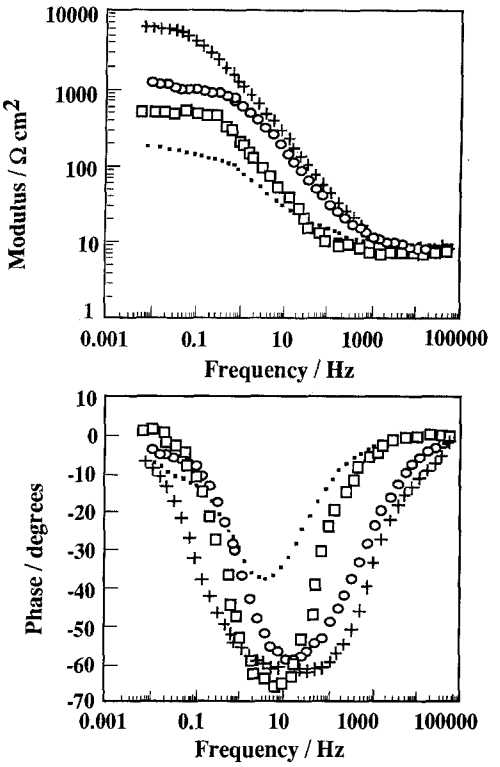

Fig. 8. Electrochemical impedance diagrams plotted in Bode coordinates obtained at pH 9 in the presence of: (□) ATMP; (○) $ZnCl_2$; (+) the inhibitive mixture; (■■■■) without inhibitor.

These observations show the intensification of the inhibitive action of the mixture due to the combined action of the compounds.

In the previous work [2], it was shown that in the presence of the mixture for a pH of 7, steady-state current–voltage curves and impedance diagrams are independent of the rotation rate of the electrode, showing that the inhibitor forms a compact layer.

The results obtained by surface analysis (XPS and IR) have been published previously [2]. The aim was to identify the compounds constituting the inhibitive

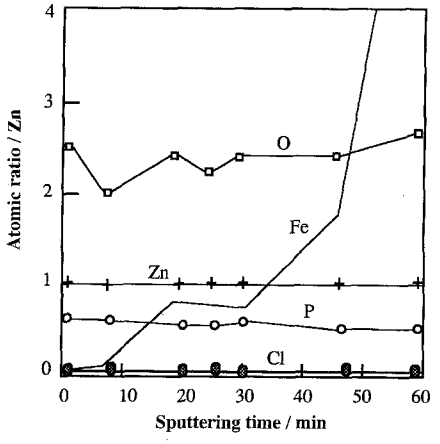

Fig. 9. XPS composition depth profile of the surface film.

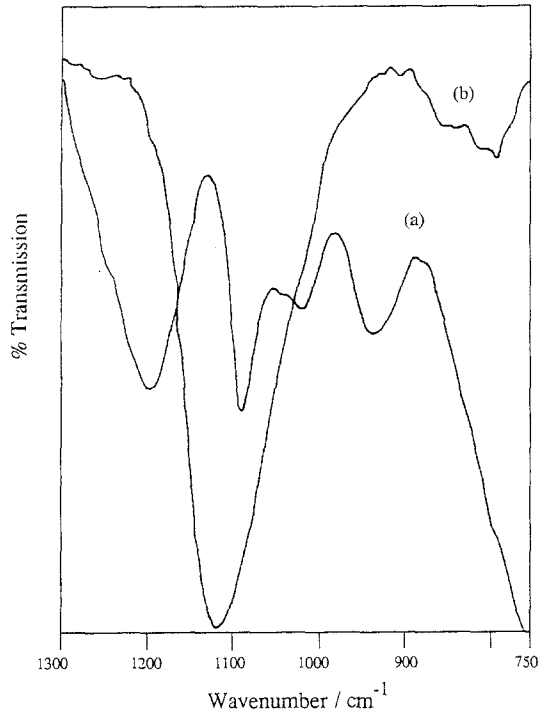

Fig. 10. (a) Infrared transmission spectrum of the solution containing the inhibitor mixture; (b) infrared reflection–absorption spectrum of the film formed on the steel substrate after immersion in the solution containing the inhibitor mixture.

layer. Some results are reported here to clarify the synergism effect.

Figure 9 shows a depth profile of Fe, Zn, P, Cl and O ratios obtained by XPS. The carbon steel sample was immersed for 17 h in the 0.5 M NaCl solution containing 500 mg dm^{-3} of the inhibitor mixture. Sputtering of the surface was used to determine the elements constituting the film as a function of the depth. The proportions of the elements were nearly constant during the sputtering. Figure 9 shows that the inhibitor film is homogeneous in composition throughout its thickness. After 90 min sputtering, only the iron peak was observed; the elements making up the protective layer had disappeared. The sputtering conditions used and the depth profile obtained suggest that the film is very thin.

A significant quantity of oxygen and zinc were present in the film. In agreement with the fact that the inhibition is largely due to the presence of zinc chloride, the protective layer is thought to be composed of $Zn(OH)_2$ resulting from the inhibition mechanism, as previously mentioned. The presence of phosphorus in the layer shows that the ATMP molecule takes part in the inhibition process.

The reflection–absorption spectrum of the film formed on polished steel is presented in Fig. 10(b). By comparison with the bulk mixture spectrum (Fig. 10(a)), a significant increase in the relative intensity of the band is observed in the region of 1100 cm^{-1}. The band at 930 cm^{-1}, due to P-OH stretching [13], almost disappears. This result was interpretated by interactions of free P-O$^-$ with metallic species to form P-O-Me bonds. Carter *et al.* [14] found infrared spectra obtained with an organic phosphate on a steel substrate that were consistent with a reaction of the phosphate with the steel to produce a metal salt. From the XPS analysis of our sample, the band at 1100 cm^{-1} was attributed to P-O-Zn bonds. This is in agreement with the fact that the band at 930 cm^{-1} is weak. Nevertheless, it is assumed that P-O-Fe bonds can occur.

According to the electrochemical results obtained at different pH values in the presence of each compound it can be concluded that:

(i) ATMP brings about a relative protection against steel corrosion. The inhibitive action is improved for more basic solutions. This is a consequence of the chelation of Fe^{2+} by the ATMP molecule. When the pH increases, formation of the complex is favoured and corrosion is slowed down. This mechanism explains the anodic action of the compound.

(ii) Zinc chloride gives an insufficient protection to the metal surface. The best protection was

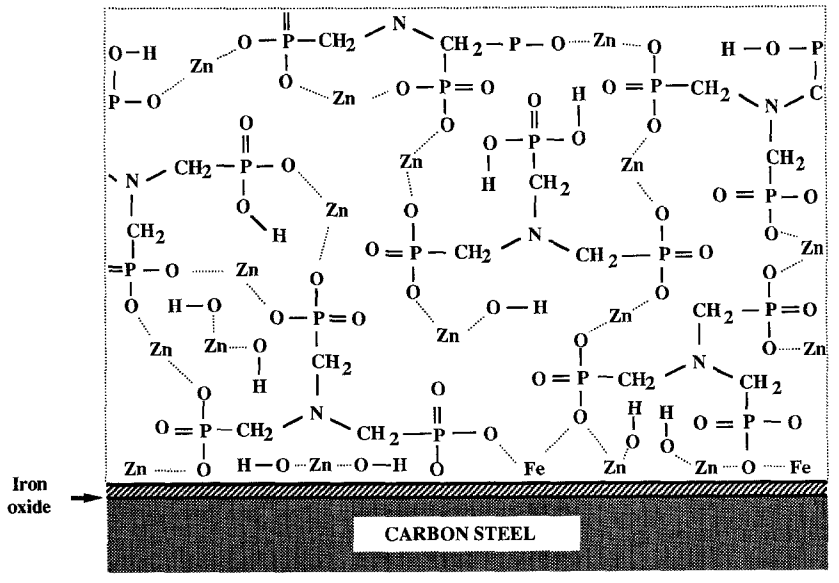

Fig. 11. Schematic representation of the inhibitive layer formed on the steel surface.

Table 4. Values of the stability constant between ATMP and various metal ions

Metal ions	$\log K_e$
Ca^{2+}	7.05
Mg^{2+}	7.2
Fe^{3+}	14.6
Zn^{2+}	16.37

obtained at pH 7 and 8. It acts as a cathodic inhibitor by precipitation in the form of zinc hydroxide caused by the local alkalinization due to oxygen reduction. The layer formed acts as a barrier for oxygen diffusion towards the metal. This layer is dissolved when the pH of the solution exceeds 9.

For the mixture, the electrochemical results show that the inhibitive efficiency is higher than that obtained with ATMP alone. This means that zinc chloride plays a role, but not the same as that observed when it is alone, because the very low current densities and the shift of the corrosion potential in the anodic direction make the pH conditions unsuitable for precipitation of the hydroxide. This compound appears at a more cathodic overvoltage in the form of a second plateau current (Fig. 5) which is not very sensitive to the hydrodynamic conditions [2].

XPS analysis indicated a constant concentration of zinc in the protective layer and infrared spectroscopy showed the existence of bonds between zinc and ATMP. Therefore, electrochemical results and surface analysis explain the synergistic effect as the formation of a zinc complex on the metal surface. A schematic representation of the layer formed on the steel surface is proposed in Fig. 11. The formation of chelate compounds with zinc ions leads to the enhancement of the corrosion protection owing to the construction of a dense system which prevents the penetration of aggressive species.

This mechanism is in agreement with the values of the stability constant, $\log K_e$, (K_e being the equilibrium constant) for the complexes formed between ATMP and different metallic ions [15, 16] (Table 4). Comparison of the stability constants gives an indication of the quantity of metal ion which is chelated. The higher the stability constant, the lower the quantity of free ions. From Table 4, it is shown that ATMP is easily able to chelate a significant quantity of zinc. This accounts for the beneficial association of zinc salt and phosphonic acid.

4. Conclusions

The corrosion inhibition of a carbon steel by associating a phosphonic acid with a zinc salt was studied with electrochemical measurements and analytical techniques. The following points can be emphasized:

(i) From the polarization curves and a.c. impedance measurements obtained in the presence of ATMP, $ZnCl_2$ and a mixture of the two, the synergistic effect is clearly shown.

(ii) ATMP alone acts as an anodic inhibitor whereas zinc chloride acts cathodically. The mixture has a mixed effect.

(iii) The infrared spectrum obtained on steel is consistent with reaction of the phosphonic acid with the zinc salt and explains the synergistic effect observed. A relatively thin and compact film is formed on the steel surface.

References

[1] M. C. Lafont, N. Pebere, F. Moran and P. Bleriot, *Revue des Sciences de l'eau*, **6** (1993) 97.

[2] Y. Gonzalez, M. C. Lafont, N. Pebere, G. Chatainier, J. Roy and T. Bouissou, *Corros. Sci.* **37** (1995) 1823.

[3] M. Duprat, M. C. Lafont and F. Dabosi, *Electrochim. Acta* **30** (1985) 353.

[4] T. Galkin, V. A. Kotenev, M. Arponen, O. Forsen and S. Ylasaari, Proceedings of the 8th European Symposium on Corrosion Inhibitors (8SEIC), Vol. 1, *Ann. Univ. Ferrara, N.S., Sez. V* (1995) 475.

[5] G. Gunasekharan, B. V. Apparao and N. Palaniswamy, *ibid.* (1995) 435.

[6] M. Duprat, N. Bui and F. Dabosi, *J. Appl. Electrochem.* **8** (1978) 455.

[7] D. You, N. Pebere and F. Dabosi, *Corros. Sci.* **34** (1993) 5.

[8] G. Levich, 'Physicochemical Hydrodynamics', Prentice-Hall, Englewood Cliffs, NJ Jersey (1962).

[9] A. Bonnel, F. Dabosi, C. Deslouis, M. Duprat, M. Keddam and B. Tribollet, *J. Electrochem. Soc.* **130** (1983) 753.

[10] J. Kubicki, P. Falewicz and S. Kuczkowska, Proceedings of the 7th European Symposium on Corrosion Inhibitors (7SEIC), Vol. 2, *Ann. Univ. Ferrara, N.S., Sez. V* (1990) 611.

[11] E. Kalman, B. Varhegyi, I. Bako, I. Felhosi, F. H. Karman and Shaban, *J. Electrochem. Soc.* **141** (1994) 3357.

[12] M. L. Hitchman, G. Meldrum, W. T. Tsai and F. C. Walsh, *Corros. Sci.* **36** (1994) 1237.

[13] N. B. Colthup, L. H. Daly and S. E. Wiberley, 'Introduction to Infrared and Raman Spectroscopy', 3rd edn, Academic Press, New York (1990).

[14] R. A. Carter III, C. A. Gierczak and R. A. Dickie, *Appl. Spectrosc.* **40** (1986) 649.

[15] S. S. Morozova, L. V. Nikitina, N. M. Dyatlova and G. V. Serebryakov, *Zhurnal Neorganicheskoi Khimii* **20** (1975) 413.

[16] H. S. Hendrickson, *Anal. Chem.* **39** (1967) 998.